Electronic Supplementary Material (ESI) for RSC Advances.

[Supporting Information]

Inorganic dye-sensitized solar cell employing In-enriched Cu-In-S ternary colloids prepared in water media

Shinya Higashimoto[a]*, Shigeki Inui[a], Takuto Nakase, Masashi Azuma[a],

Mari Yamamoto[b] and Masanari Takahashi[b]

[a] *College of Engineering, Osaka Institute of Technology, 5-16-1 Omiya, Asahi-ku, Osaka 535-8585, Japan*

[b] Osaka Municipal Technical Research Institute, 1-6-50 Morinomiya, Joto-ku, Osaka 536-0025, Japan

To whom correspondence should be addressed.

Dr. Shinya Higashimoto

Tel: +81-6-6954-4283; fax: +81- 6-6957-2135; E-mail: higashimoto@chem.oit.ac.jp

In order to characterize the oxidative states of the chemical compositions in the photo-electrode, the X-ray Photoelectron Spectroscopic (XPS) measurements were performed with a KRATOS, AXIS Ultra spectrometer using Al K_α radiation (E = 1486.8 eV). As shown in **Fig. SI 1**, the XPS spectrum of Cu 2p is split into two peaks centered at 932.8 eV for Cu $2p_{3/2}$ and 952.5 eV for Cu $2p_{1/2}$ due to the Cu^+ ions[1], while the satellite peak of Cu^{2+} centered at 942 eV cannot be observed.[2] Therefore, the Cu^{2+} ions have been probably reduced by thioglycolic acid (TGA) to form Cu^+ ions. The In 3d XPS spectrum is split into two peaks centered at 444.2 eV for In $3d_{5/2}$ and at 452.0 eV for In $3d_{3/2}$ peak. Moreover, the S 2p XPS spectrum can be deconvoluted into two gaussian peaked at 161.9 eV for Cu–S and at 163.1 eV for In–S, which is in good agreement with the previous report.[3]

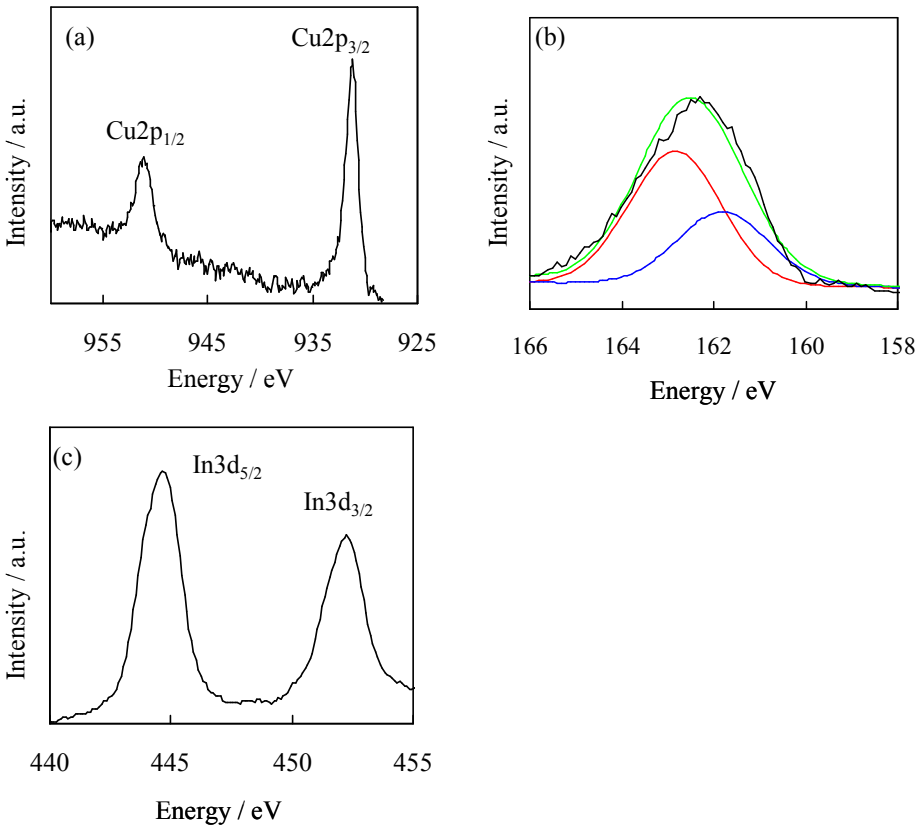

Fig. SI 1 XPS spectra of Cu (a), S (b) and In (c) of the CIS123-TiO_2.

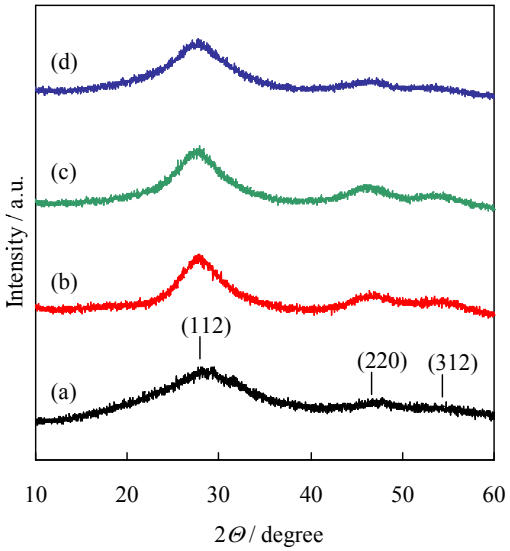

Fig. SI 2 XRD patterns of CIS colloids: In/Cu = 1 (a), 2 (b), 3 (c) and 4 (d). XRD analysis shows broad diffraction patterns at 2Θ values of 27.7, 46.6 and 55.2°, corresponding to the (112), (220) and (312) indices, respectively, of the tetragonal CIS crystal structure (JCPDS card 47-1372). No other additional phases such as In_2S_3 were observed.

It is known that the quantum size confinement effects of semiconductor appear from the particle sizes less than ca. 10 nm. The upper limit of the particle diameter for the quantum confinement is approximately given by the Bohr radius. According to the previous report,[4] the Bohr radius of $CuInS_2$ (CIS) was estimated to be 4.4 nm. Since the size of CIS colloidal particles are in the range of ca. 2 ~ 4 nm prepared in this study, it can be assumed that these colloidal particles exhibit the quantum size confinement effects.

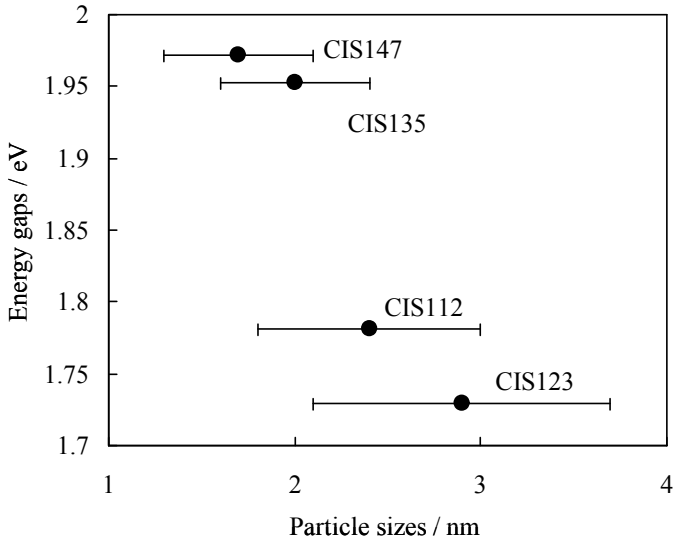

Fig. SI 3 Relationship between particle sizes of CIS colloids and energy gaps.

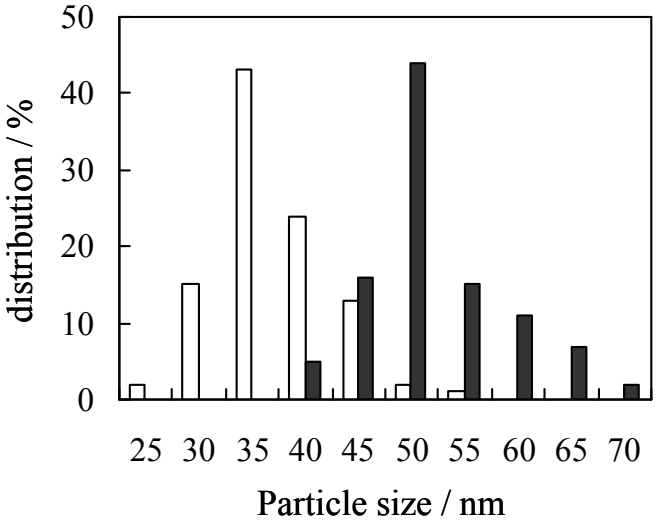

Fig. SI 4 Distribution of particle sizes of TiO_2 (white bar) and CIS123-TiO_2 (black bar).

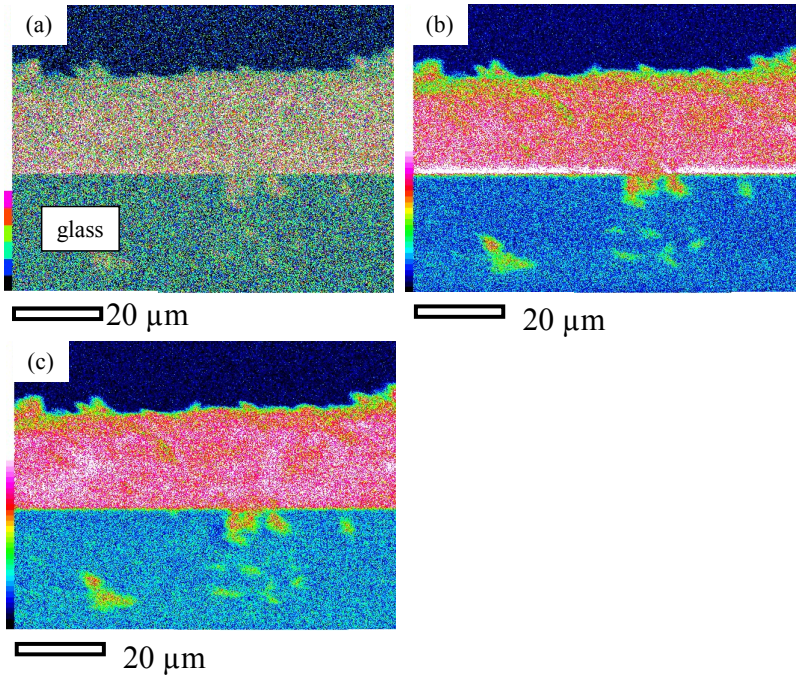

Fig. SI 5 Elemental mappings of Cu (a), In (b) and S (c) on the CIS123-TiO_2 through the cross section.

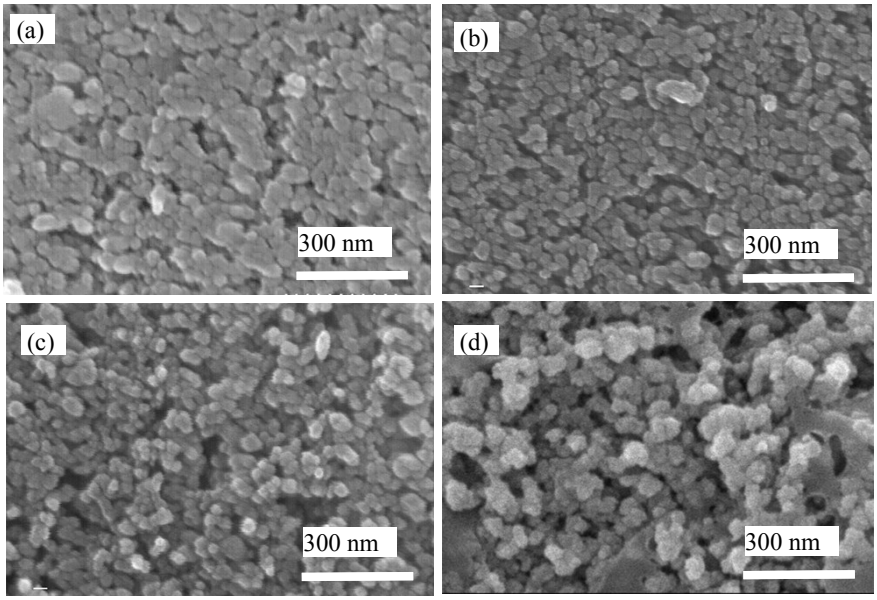

Fig. SI 6 FE-SEM images of CIS112-TiO_2 (a), CIS135-TiO_2 (b), CIS147-TiO_2 (c), and ZnS(6)/CIS123-TiO_2 (d).

Characteristic XRD patterns attributed to the CIS particles in several CIS-TiO_2 and ZnS/CIS-TiO_2 electrodes were not clearly detected (See Fig. SI 7), suggesting that the CIS particles are highly dispersed on the TiO_2. Moreover, the ZnS on ZnS(6)/CIS123-TiO_2 was found to form an amorphous structure.

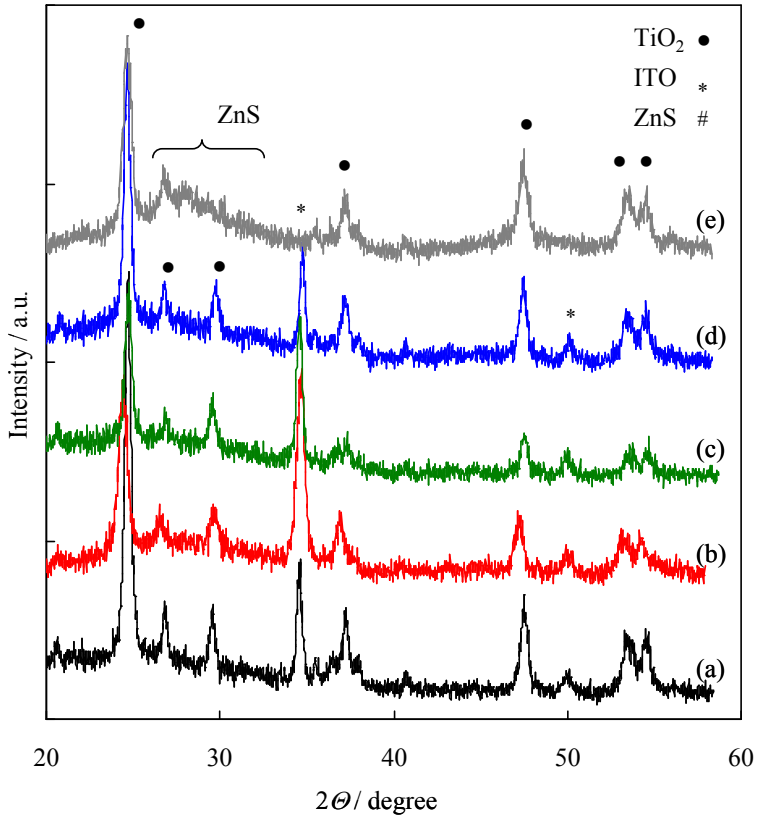

Fig. SI 7 XRD patterns of CIS112-TiO_2 (a), CIS123-TiO_2 (b), CIS135-TiO_2 (c), CIS147-TiO_2 (d) and ZnS(6)/CIS123-TiO_2 (e).

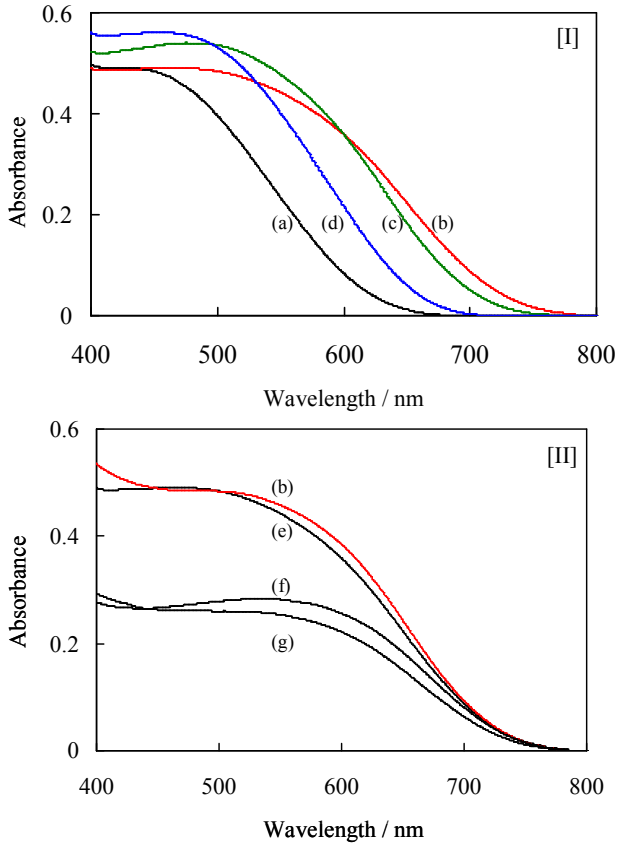

Fig. SI 8 UV-Vis spectra of [I] CIS112-TiO_2 (a), CIS123-TiO_2 (b), CIS135-TiO_2 (c), CIS147-TiO_2 (d) and [II] ZnS(2)/CIS123-TiO_2 (e), ZnS(6)/CIS123-TiO_2 (f), ZnS(8)/CIS123-TiO_2 (g).

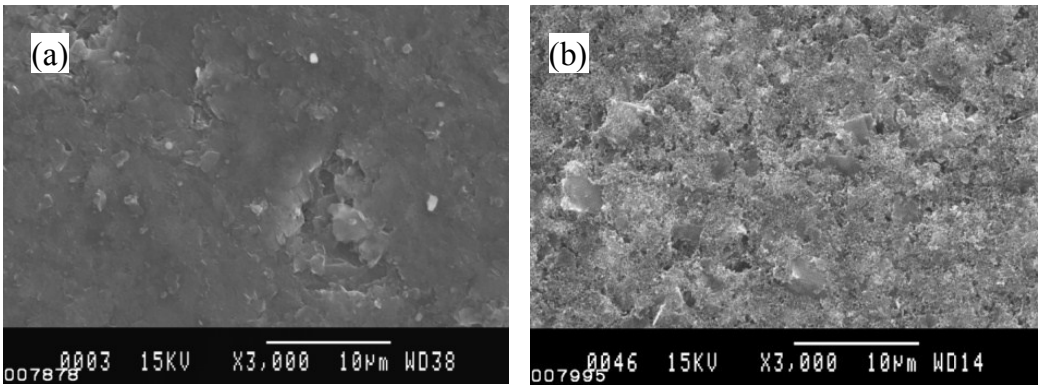

Fig. SI 9 SEM images of graphite electrode (a) and its surface modification with porous carbon (b).

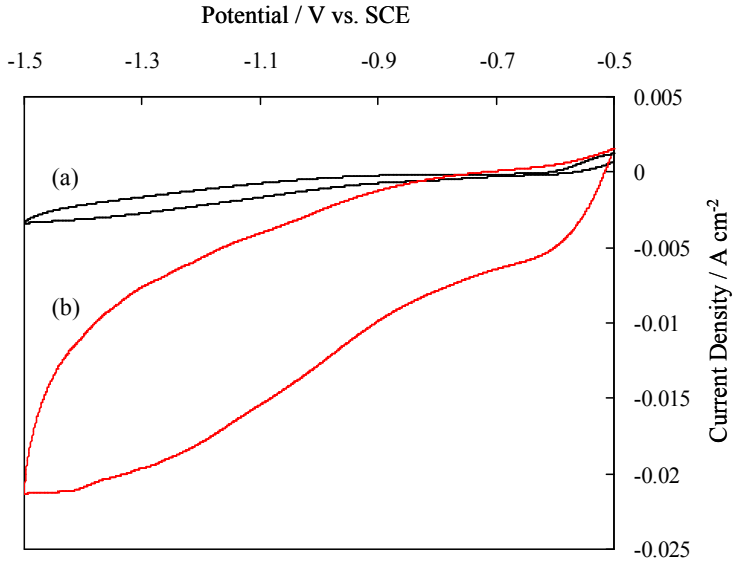

Fig. SI 10 Cyclic voltammogram of graphite electrode (a) and its surface modification with porous carbon (b). The cyclic voltammogram was obtained in the scan rate at 10 mV/sec using three electrodes: carbon electrode for working electrode, Pt wires for auxiliary and Ag/AgCl for reference electrode.

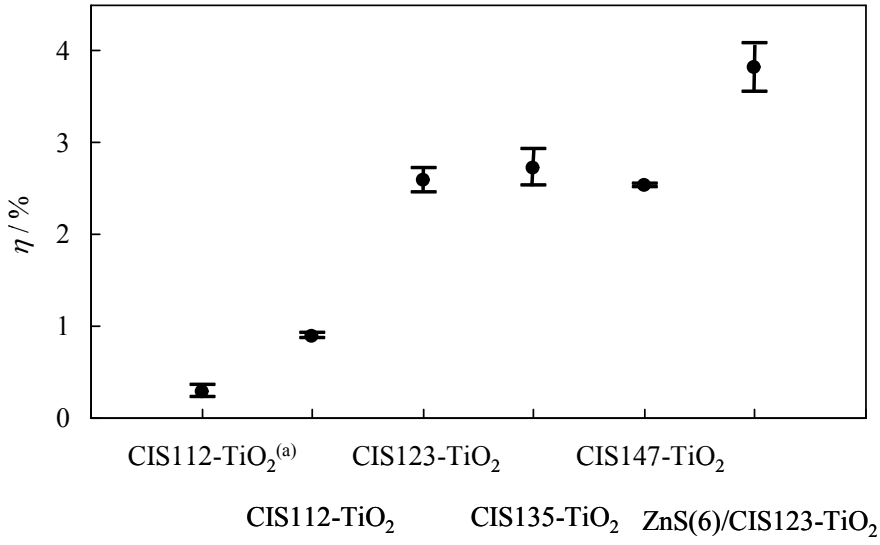

Fig. SI 11 Reproducibility of the PCE for several CIS-TiO_2 photoelectrodes using carbon electrode with carbon modification. (a) Counter electrode was employed with graphic carbon.

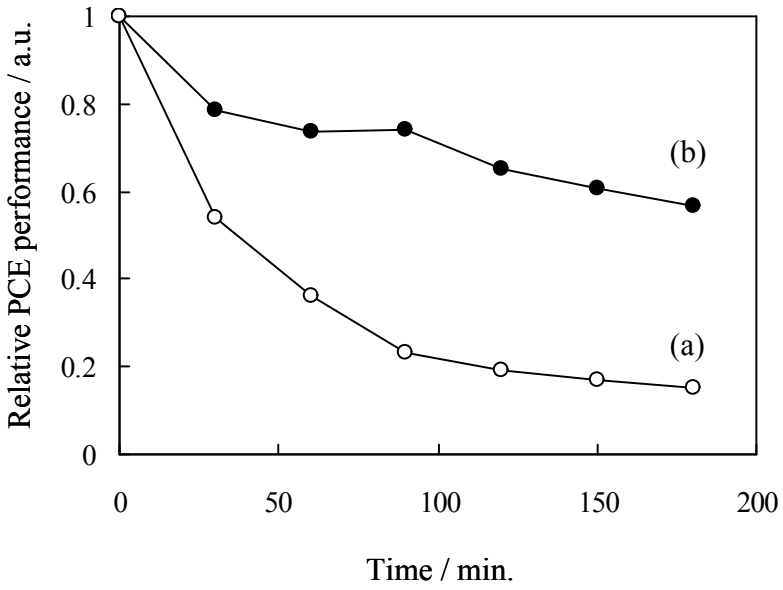

Fig. SI 12 Relative photo-stabilities of CIS123-TiO_2 (a) and ZnS(6)/CIS123-TiO_2 (b).

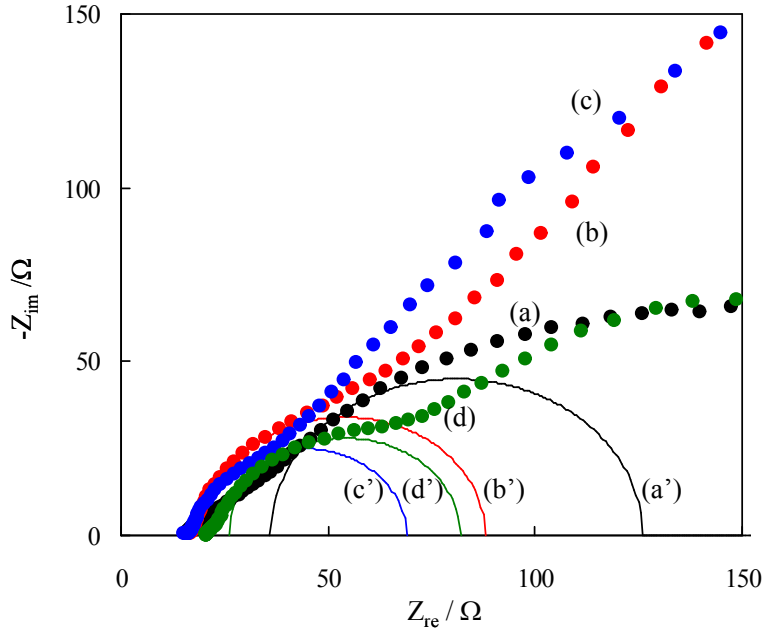

Fig. SI 13 Nyquist plots for the CIS112-TiO_2 (a, a'), CIS123-TiO_2 (b, b'), CIS135-TiO_2 (c, c') and CIS147-TiO_2 (d, d') and their corresponding semi-circles (a' ~ d').

References

1 S. Li, Z. Zhao, Q. Liu, L. Huang, G. Wang, D. Pan, H. Zhang and X. He, *Inorg. Chem.,* 2011, **50**, 11958.
2 L. D. Partain, R. A. Schneider, L. F. Donaghey, P. S. Mcleod, *J. Appl. Phys.,* 1985, **57**, 5056.
3 J. Xiao, Y. Xie, R. Tang, Y. Qian, J. Solid State Chem., 2001, 161, 179.
4 M. J. Anc, N. L. Pickett, N. C. Gresty, J. A. Harris, K. C. Mishra, *e-J. Surf. Sci. Technol*., 2013, **2**, R3071.